The Astrophysical Journal, 831:96 (16pp), 2016 November 1 doi:10.3847/0004-637X/831/1/96
© 2016. The American Astronomical Society. All rights reserved.

UNCOVERING CIRCUMBINARY PLANETARY ARCHITECTURAL PROPERTIES FROM SELECTION BIASES

Gongjie Li[1], Matthew J. Holman[1], and Molei Tao[2]
[1] Harvard-Smithsonian Center for Astrophysics, The Institute for Theory and Computation, 60 Garden Street, Cambridge, MA 02138, USA
[2] School of Mathematics, Georgia Institute of Technology, 686 Cherry Street, Atlanta, GA 30332, USA; mtao@gatech.edu
Received 2016 March 30; revised 2016 August 2; accepted 2016 August 4; published 2016 October 28

ABSTRACT

Studying newly discovered circumbinary planetary systems improves our understanding of planetary system formation. Learning the architectural properties of these systems is essential for constraining the different formation mechanisms. We first revisit the stability limit of circumbinary planets. Next, we focus on eclipsing stellar binaries and obtain an analytical expression for the transit probability in a realistic setting, where a finite observation period and planetary orbital precession are included. Our understanding of the architectural properties of the currently observed transiting systems is then refined, based on Bayesian analysis and a series of tested hypotheses. We find that (1) it is not a selection bias that the innermost planets reside near the stability limit for eight of the nine observed systems, and this pile-up is consistent with a log uniform distribution of the planetary semimajor axis; (2) it is not a selection bias that the planetary and stellar orbits are nearly coplanar ($\lesssim 3^\circ$), and this —along with previous studies—may imply an occurrence rate of circumbinary planets similar to that of single star systems; (3) the dominance of observed circumbinary systems with only one transiting planet may be caused by selection effects; (4) formation mechanisms involving Lidov–Kozai oscillations, which may produce misalignment and large separation between planets and stellar binaries, are consistent with the lack of transiting circumbinary planets around short-period stellar binaries, in agreement with previous studies. As a consequence of (4), eclipse timing variations may better suit the detection of planets in such configurations.

Key words: binaries: eclipsing – celestial mechanics – planetary systems

1. INTRODUCTION

Investigation of newly discovered circumbinary planetary systems can provide better understanding of planetary formation. To date, 11 transiting circumbinary planets have been discovered, residing in nine planetary systems, including: Kepler-16b (Doyle et al. 2011); Kepler-34b and 35b (Welsh et al. 2012); Kepler-38b (Orosz et al. 2012a); Kepler-47b, 47c, (Orosz et al. 2012b) and 47d (Hinse et al. 2015, J. A. Orosz et al. 2016, in preparation); Kepler-64b (Kostov et al. 2013; Schwamb et al. 2013); Kepler-413b (Kostov et al. 2014); Kepler-453b (Welsh et al. 2015); and Kepler-1647b (Kostov et al. 2015). Many of them share interesting architectural features. For instance, the locations of the planets are mostly near the stability limit, the mutual inclinations between the planetary orbits and the stellar binary orbits are low, and the planets preferentially orbit around stars with long stellar orbital periods.

The architectural properties of these systems reveal important clues to the origin of circumbinary planetary systems. For instance, the observed pile-up of planets near the stability limit may indicate the dominance of disk migration, as the planets move toward the instability limit, via disk migration, from their birth location—which is likely farther away (e.g., Paardekooper et al. 2012; Marzari et al. 2013; Pierens & Nelson 2013; Rafikov 2013; Kley & Haghighipour 2014; Bromley & Kenyon 2015; Silsbee & Rafikov 2015). In addition, the near-coplanar configuration of the circumbinary planetary systems around closely separated binary stars is consistent with theoretical studies of the gravitational torque between the binary and the circumbinary disk, which produces the alignment (Foucart & Lai 2013, 2014). Moreover, the coplanarity is also consistent with the observed alignment of protoplanetary disks around young binary stars (Rosenfeld et al. 2012; Czekala et al. 2015, 2016), and with the debris disks around short-period binaries (Kennedy et al. 2012b). This may imply a primordial origin of the alignment of their planetary orbits. Note that 99 Herculis hosts a misaligned circumbinary debris disk, and the origin of its misalignment challenges the collisional and dynamical evolution of the system (Kennedy et al. 2012a).

Some of the architectural features are caused by dynamical interactions that play critical roles in the origin of the planetary systems. Hierarchical three-body system dynamics has been studied extensively in the literature. In the case when the inner binary contains of a test particle, the eccentricity and inclination of the inner binary can oscillate, due to the perturbation of the outer object under the Lidov–Kozai mechanism (Kozai 1962; Lidov 1962). Including the octupole order of expansion (third power in the semimajor axis ratio), it has been shown that the inner orbit can change from a prograde orbit to a retrograde one, and the eccentricity can be excited very close to unity (e.g., Katz et al. 2011; Naoz et al. 2011; Li et al. 2014). In the case when the outer object is a test particle, which is more relevant to the circumbinary planets, the Lidov–Kozai oscillations disappear (Migaszewski & Goździewski 2011; Martin & Triaud 2016). On the other hand, multiple equilibria exist when the mutual inclination is high (Palacián & Yanguas 2006; Verrier & Evans 2009; Farago & Laskar 2010; Doolin & Blundell 2011). In addition, the orbit of the test particle is not stable when it is very close to the binary. Stability limits have been obtained for large-parameter spaces (e.g., Dvorak et al. 1989; Holman & Wiegert 1999; Musielak et al. 2005; Doolin & Blundell 2011), and outcomes of the unstable systems have been investigated (Sutherland & Fabrycky 2015; Smullen et al. 2016).

In addition to the dynamical effects, selection biases also influence the observed architectural properties. Thus, correcting selection biases is crucial when extracting the architectural

properties from observed circumbinary systems. For instance, the detection limitation favors planets that are closer to the stellar binaries, and it is more likely to detect planets that are coplanar with the eclipsing stellar binaries using the transit method. Considering selection effects, Armstrong et al. (2014) studied the abundances and properties of circumbinary systems extensively, using the approach of population synthesis. They found that the occurrence rate of circumbinary planetary systems has a lower limit of 47%, if the mutual inclination between the planetary orbit and the stellar binary is isotropically distributed. This implies that the circumbinary systems are preferentially coplanar, or can be formed much more easily than the single star systems. However, precession was neglected in the previous derivation of the occurrence rate, and it has been shown that precession plays an important role in the transit probability (Schneider 1994; Martin & Triaud 2015). In particular, Martin & Triaud (2015) show that, if one takes an infinite amount of time, the transit probability for a circumbinary planetary system is larger than that of a single star system, and the transit probability increases with mutual inclination. It is not realistic to consider an infinite amount of observation time, yet the transit probability over a finite observation time has not been derived analytically. Here, we revisit the transit probability to derive the transit probability in a finite observation time and include orbital precession for planets orbiting eclipsing binaries. We then correct selection biases using transit probabilities, in order to obtain the architectural properties of the observed circumbinary planetary systems. This differs from Martin & Triaud (2014), who considered selection biases for planets orbiting both eclipsing and non-eclipsing binaries, using a large number of synthetic systems based on *N*-body simulations. Specifically, they found that the pile-up of the planets near the stability limit is not due to selection biases, and the coplanarity of the systems may indicate either a high occurrence rate of circumbinary systems, or that the coplanarity is not a selection effect. In this article, we focus on the observed systems, and use Bayesian analysis to study the selection effects. For instance, the coplanarity is not degenerate with the occurrence rate of the circumbinary planetary systems this way.

This article is organized as follows. In Section 2, we revisit the stability of the circumbinary planets, including high mutual inclinations between the orbits of the planet and stellar binary. In Section 3, we provide an analytical expression for the transit probability, in a finite observational period, as a function of stellar and planetary orbital parameters. We conclude with Section 4, wherein we study the circumbinary architecture corrected from selection biases, using the transit probability.

2. STABILITY LIMIT AS A FUNCTION OF MUTUAL INCLINATION

The stability of circumbinary systems has been studied (e.g., Dvorak et al. 1989; Holman & Wiegert 1999; Pilat-Lohinger et al. 2003; Musielak et al. 2005; Doolin & Blundell 2011). In particular, Doolin & Blundell (2011) discussed many interesting features of the parameter space where such systems are stable, extending mutual inclination between the orbits of the stellar binary and the planet from 0° to 180°, including eccentric stellar binaries and different stellar mass ratios, assuming the planet is massless. It has been found that the retrograde orbits are more stable than the prograde orbits, which is true for three-body problems in general. In addition, there exist striations of instability, likely due to resonances between the stellar binary and the planet, and there are pinnacles and peninsulas of unstable regions for the non-librating and librating regions, respectively, except when the stellar masses are equal.

The critical semimajor axis, within which the planet is unstable for the coplanar case, was obtained by Holman & Wiegert (1999). They performed a large number of numerical simulations that cover a wide range of stellar binary eccentricity and stellar mass ratio. For reference, a_c is expressed as the following:

$$\begin{aligned} a_c = [&(1.60 \pm 0.04) + (5.10 \pm 0.05)e \\ &+ (-2.22 \pm 0.11)e^2 + (4.12 \pm 0.09)\mu \\ &+ (-4.27 \pm 0.17)e\mu + (-5.09 \pm 0.11)\mu^2 \\ &+ (4.61 \pm 0.36)e^2\mu^2]a_b, \end{aligned} \quad (1)$$

where e is the stellar binary eccentricity, $\mu = m_2/(m_1 + m_2)$ is the stellar mass to total stellar mass ratio, and a_b is the stellar binary semimajor axis. The expression is obtained by fitting the results of the numerical simulations, and the uncertainties are inherent from the fit. Note that this stability limit works only for the coplanar cases. Because discussions will include the misaligned cases, in the next sections, here, we first illustrate the stability limit and the marginally stable parameter space as a function of the mutual inclination.

To study the stability limit when the planetary orbit is misaligned, we performed a large number of numerical integrations. For simplicity, we set the stellar masses to be one solar mass, the stellar orbit to be circular, and the planet mass to be a Jupiter mass. We include simulations with different planetary semimajor axes and the mutual inclinations. For each planetary semimajor axis and mutual inclination, we run eight simulations with different planetary orbital phase angles equally spaced by $\pi/4$, and we stop the runs after 10^5 stellar binary periods. We use a fourth-order symplectic integrator (see, e.g., Forest 1989; Suzuki 1990; Yoshida 1990; McLachlan & Quispel 2002; Tao & Owhadi 2016) to obtain the trajectory of the stars and the planets, and we check that the energy change fraction is sufficiently small ($\lesssim 10^{-8}$).

Figure 1 shows the results of the simulations. The upper panel shows the fraction of survived (stable) systems as a function of initial planetary semimajor axis and mutual inclination. We record that a system is survived (or is stable) when there is no collision and a_p remains within 3 AU. The lower panel shows the probability that the change in planetary semimajor axis is less than 10% of its initial value ($\delta a < 0.1a_0$) to illustrate the marginally stable region. We find that, at higher mutual inclinations, the planetary systems are more stable overall. This is consistent with the results of Wiegert & Holman (1997), who studied the stability of planets in Alpha centauri, and with Doolin & Blundell (2011). Note that instability islands due to resonances can occur at high mutual inclination, when the semimajor axis of the planet still remains outside the coplanar stability limit, and moderate semimajor axis variations exhibit interesting phase space dependence. Further analysis on these topics is important, but outside the scope of this article. Because misaligned orbits are also stable inside the stability limit, we use the stability limit, as defined in Equation (1), derived by Holman & Wiegert (1999) for the coplanar case, for the following sections.

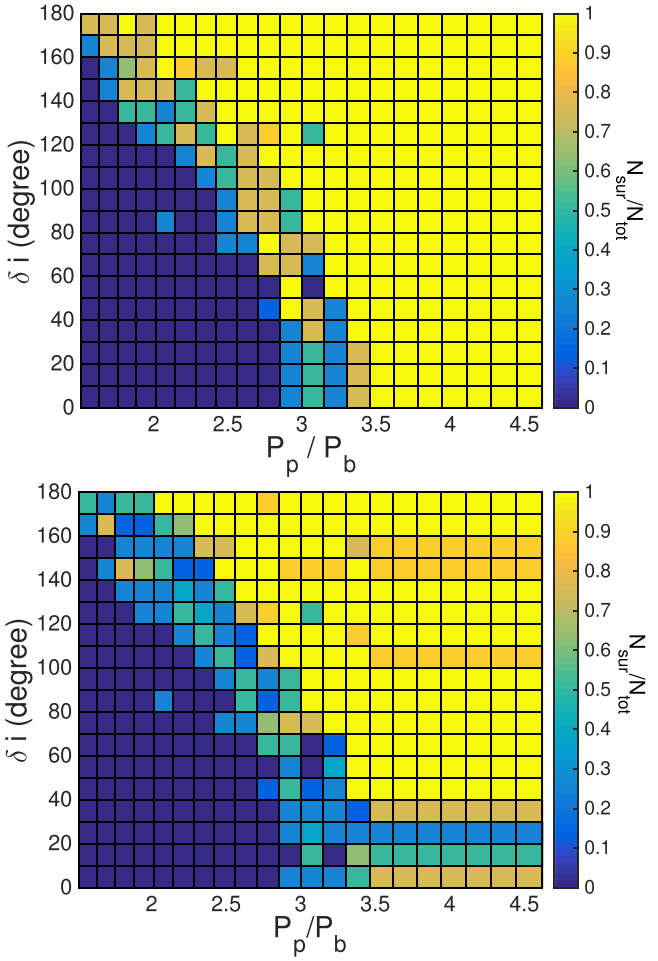

Figure 1. Probability that a system can survive (upper panel) and $\delta a < 0.1 a_0$ (lower panel), as a function of planetary orbital period to stellar orbital period ratio and mutual inclination. The stellar orbital period is five days, the mass of the stars equals one solar masses, and the mass of the planet is 0.001 solar mass. Systems are more stable when the mutual inclination is higher.

3. TRANSIT PROBABILITY

Understanding transit probability is important for correcting selection effects, in order to obtain the architectural properties of circumbinary planetary systems. Because the circumbinary systems observed so far only involve eclipsing stellar binaries, we focus on eclipsing stellar binaries in this article. In this section, we first derive the analytical expression of the transit probability for a finite observation period, taking orbital precession into account. We then check the analytical expression with numerical simulations.

3.1. Analytical Expression

The configuration of the system is shown in Figure 2, where we align the x-axis with the line of sight, and set the z-axis to be in the plane of the angular momentum of the stellar binary and the line of sight. The axis of z' is aligned with the angular momentum of the stellar binary, and the stellar orbit lies in the plane of $x' - y$. In other words, by rotating the x-axis and the z-axis along the y-axis by the angle $\Delta_{ib} = 90° - i_b$, one can separately obtain the x' axis and the z' axis, where i_b is the line-of-sight inclination of the stellar orbit. Here, m_1 and m_2 stand for the masses of the stars, and m_p for the mass of the planet. The symbol Ω denotes the longitude of ascending node of the

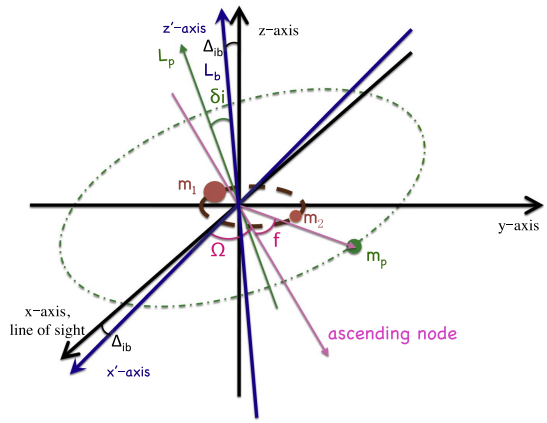

Figure 2. The configuration of the circumbinary system, where m_1 and m_2 stand for the stellar binary, m_p stands for the planet, and δi represents the mutual inclination between the orbits of the planet and the stellar binary.

planet with respect to the $x' - y$ plane, f denotes the true anomaly of the planet, and δi denotes the mutual inclination between the planetary orbit and the stellar binary orbit. Note that we only focus on eclipsing stellar binaries, and thus, Δ_{ib} is very small. In the limit of a circular planetary orbit with semimajor axis (a_p), the x, y, and z components of the coordinate of the planet can be expressed as the following:

$$x_p = a_p(\sin(f)\sin(\delta i)\sin(\Delta_{ib}) + (\cos(\Omega)\cos(f) - \sin(\Omega)\sin(f)\cos(\delta i))\cos(\Delta_{ib})) \quad (2)$$

$$y_p = a_p(\sin(\Omega)\cos(f) + \cos(\Omega)\sin(f)\cos(\delta i)) \quad (3)$$

$$z_p = a_p(\sin(f)\sin(\delta i)\cos(\Delta_{ib}) - (\cos(\Omega)\cos(f) - \sin(\Omega)\sin(f)\cos(\delta i))\sin(\Delta_{ib})). \quad (4)$$

With precession, it is difficult to directly characterize the parameter space that allows transits. Thus, we separate the transit criterion into two parts. Specifically, we first use the geometrical approach to obtain a criterion for the planets to transit the stellar binary orbit. We then use a probabilistic approach to estimate how often the planet transits the star. This differs from Martin & Triaud (2015), who considered only the first part, deriving an analytic criterion for orbital crossings, and showed numerically that this guaranteed transits—but only with infinite observing time.

To cross the stellar orbit, the line-of-sight projection of the planet is required to lie within that of the stellar orbit. Specifically, the y-component of the planet position needs to be smaller than the semimajor axis of the star ($|y_p| < a_{b,1}$); the x-component of the planet position needs to be positive; and, in the limit where the stellar binary is eclipsing (i.e., Δ_{ib} is small), the z-component of the planet position needs to be smaller than the radius of the star ($|z_p| < R_{*,1}$). In the first order of Δ_{ib} and δi, the condition to cross the orbit of m_1 is expressed below:

$$x_p \sim a_p(\cos(\Omega + f)) > 0, \quad (5)$$

$$|y_p| \sim a_p|\sin(\Omega + f)| < a_{b,1}, \quad (6)$$

$$|z_p| \sim a_p| - \cos(\Omega + f)\Delta_{ib} + \sin(f)\delta i| < R_{*,1}. \quad (7)$$

where $a_{b,1} = a_b m_2/(m_1 + m_2)$, a_b is the semimajor axis of the stellar binary orbit, a_p is the semimajor axis of the planetary

orbit, and $R_{*,1}$ is the radius of star 1. We assume the orbits are circular, for simplicity. The expression is interchangeable for m_2. In the first order of a_b/a_p, (5)–(7) can be expressed as:

$$-a_{b,1}/a_p < \sin(\Omega + f) < a_{b,1}/a_p, \tag{8}$$

$$\frac{-R_{*,1}/a_p + \Delta_{ib}}{\delta i} < \sin f < \frac{R_{*,1}/a_p + \Delta_{ib}}{\delta i}. \tag{9}$$

Note that, if $-R_{*,1}/a_p + |\Delta_{ib}| > \delta i$, the planet cannot transit the star m_1.

Extending to higher δi by substituting δi with $\sin(\delta i)$ in Equations (8)–(9), we obtain a range of Ω that allows the planet to cross the stellar orbit of m_1:

$$\Delta\Omega_1 = \begin{cases} \min[2(f_2 - f_1) + 4\mathrm{asin}(a_{b,1}/a_p),\ 2\pi] \\ \quad \text{if } \pi/2 - f_2 > \mathrm{asin}(a_{b,1}/a_p) \\ \quad\quad \& f_1 + \pi/2 > \mathrm{asin}(a_{b,1}/a_p), \\ \min[2(f_2 - f_1) + 2(\pi/2 - f_2) \\ + 2\mathrm{asin}(a_{b,1}/a_p),\ 2\pi] \\ \quad \text{else if } f_1 + \pi/2 > \mathrm{asin}(a_{b,1}/a_p), \\ \min[2(f_2 - f_1) + 2(\pi/2 - f_2) + 2(f_1 + \pi/2),\ 2\pi] \\ \quad \text{else.} \end{cases} \tag{10}$$

where

$$f_1 = \begin{cases} \mathrm{asin}\left(\frac{-R_{*,1}/a_p + \sin(|\Delta_{ib}|)}{\sin(\delta i)}\right) \\ \quad \text{if } -1 < (-R_{*,1}/a_p + \sin(|\Delta_{ib}|))/\sin(\delta i) < 1, \\ -\pi/2 \\ \quad \text{else if } (-R_{*,1}/a_p + \sin(|\Delta_{ib}|))/\sin(\delta i) < -1, \\ \pi/2 \\ \quad \text{else.} \end{cases}. \tag{11}$$

and

$$f_2 = \begin{cases} \mathrm{asin}\left(\frac{R_{*,1}/a_p + \sin(|\Delta_{ib}|)}{\sin(\delta i)}\right) \\ \quad \text{if} -1 < (R_{*,1}/a_p + \sin(|\Delta_{ib}|))/\sin(\delta i) < 1, \\ -\pi/2 \\ \quad \text{else if } (R_{*,1}/a_p + \sin(|\Delta_{ib}|)/\sin(\delta i) < -1, \\ \pi/2 \\ \quad \text{else.} \end{cases}. \tag{12}$$

The difference of f_2 and f_1 contributes to the range of Ω that allows the planet to cross the stellar orbit. Note that Ω has two distinctive regions that allow transit, if $\pi/2 - f_2 > \mathrm{asin}(a_{b,1}/a_p)$, and these two regions are connected if $f_1 + \pi/2 > \mathrm{asin}(a_{b,1}/a_p)$.

Next, we take into account orbital precession to estimate the probability that the planet will cross the stellar orbit over time. Briefly, orbital precession can increase the transit probability because it broadens the range of Ω covered, increasing the likelihood of it entering the window that allows transits. Because most of the stellar binaries are not highly eccentric, we take the limit to be when $e_b \to 0$. The precession timescale ($T_{\rm prec}$) of the planetary orbit then scales with the planetary orbital period (P_p) as:

$$T_{\rm prec} = \frac{2\pi}{|\dot{\Omega}|} \tag{13}$$

$$= P_p \frac{4}{3\cos\delta i} \frac{a_p^2}{a_b^2} \frac{(m_1 + m_2)^2}{m_1 m_2}, \tag{14}$$

as obtained by Schneider (1994), who considered the precession timescale when $m_1 = m_2$. Farago & Laskar (2010) derived an equation for the more general case with eccentric binaries. Note that, when the stellar binary is eccentric, the precession is more complicated, because the longitude of node can librate around $\pm\pi/2$, when the inclination is high. When the stellar binary is circular, Ω decreases with time if the inclination is below $\pi/2$, and Ω increases with time if the inclination is above $\pi/2$. We adopt the expression of Equation (14), for simplicity, in the following analysis; i.e., Ω increases/decreases linearly with time. Specifically, the change in Ω due to precession is denoted as $\delta\Omega_{\rm prec} = \dot{\Omega} T_{\rm obs}$.

The total range of the node longitude during the observation time period ($T_{\rm obs}$) is $\delta\Omega_1 = \Delta\Omega_1 + \dot{\Omega} T_{\rm obs}$.

$$\delta\Omega_1 = \begin{cases} \Delta\Omega_1 + 2\delta\Omega_{\rm prec} \\ \quad \text{if } \pi/2 - f_2 > \delta\Omega_{\rm prec}/2 \\ \Delta\Omega_1 + \delta\Omega_{\rm prec} + 2(\pi/2 - f_2) \\ \quad \text{else if } \pi/2 - f_2 > \mathrm{asin}(a_{b,1}/a_p) \\ \Delta\Omega_1 + \delta\Omega_{\rm prec} \\ \quad \text{else} \end{cases} \tag{15}$$

The probability to cross the stellar orbit ($P_{\rm cr,1}$) for m_1 is then:

$$P_{\rm cr,1} = \frac{\min[\delta\Omega_1,\ 2\pi]}{2\pi}. \tag{16}$$

We next calculate the probability for the planet to transit the stars, given that the planet crosses the stellar orbit. It is roughly the ratio of the relative displacement of the planet and the star, as the planet crosses to the projected width of the stellar orbit. The relative displacement depends on the time it takes for the planet to cross the orbit, which can be expressed as $t_{\rm trans} \sim \pi/2(R_{*,1})/(v_p \sin\delta i)$, where v_p is the orbital velocity of the planet, and the factor $\pi/2$ corresponds to the correction—taking into account the different impact parameters to cross the star. The relative velocities of the planet and star depend on whether they are on the same side of the other star. When the planet and star are both toward the observer with respect to the center of mass ($x_p > x_* > 0$), they are moving in the same direction, and the relative displacement is roughly: $dl_1 = (t_{\rm trans}(|v_p \cos\delta i - 2v_{*,1}/\pi|) + R_{*,1})$, where $v_{*,1}$ is the orbital velocity of the star, and factor $2/\pi$ gives the averaged line-of-sight projected stellar velocity. On the other hand, when the star is on the other side of the center of mass ($x_p > 0 > x_*$), the planet and star move in the opposite directions. Thus, the relative displacement is $dl_2 = (t_{\rm trans}(|v_p \cos\delta i + 2v_{*,1}/\pi|) + 2R_{*,1})$. The projected size of the stellar orbit can be expressed as: $2a_{b,1}$. Therefore, the probability that the planet can transit in front of the

star m_1 is roughly:

$$P_{*,1} = \begin{cases} 1, & \text{if } (dl_1 + dl_2)/2 > 2a_{b,1} \\ \frac{1}{4a_{b,1}}(dl_1 + dl_2) & \text{otherwise} \end{cases}. \quad (17)$$

Note that the movements of the planet and star enhance the transit probability. Specifically, the motion of the planet is important when the mutual inclination is low, because it takes a long time for the planet to cross the stellar orbits. In addition, the relative displacement and transit probability are dominated by the motion of the stars when mutual inclination is high.

During the observation time period $T_{\rm obs}$, the planet can cross the stellar orbit multiple times, and the transit probability increases as the number of orbit crossing increases. The maximum number of crossing is $T_{\rm obs}/P_p$, which occurs when the precession is slow and the node longitude stays in the window that allows crossing (e.g., when the mutual inclination is high $\sim 90°$). In this limit, the planet crosses the stellar orbit every time. When the precession is fast, it dominates the number of stellar orbit crossing times. The number of orbit crossing is $\Delta\Omega_1/(\dot{\Omega}P_p)$, if $\pi/2 - f_2 < \mathrm{asin}(a_{b,1}/a_p)$, when the region where Ω allows transit over 2π is connected, and $\Delta\Omega_1/2/(\dot{\Omega}P_p)$ if $\pi/2 - f_2 > \mathrm{asin}(a_{b,1}/a_p)$, when the regions where Ω allows transit over 2π are separated. When the precession is even faster, the node can precess to the range that allows transit more than once. In sum, the number of stellar orbit crossings can be expressed as the following:

$$n_1 = \begin{cases} \min[\frac{T_{\rm obs}}{P_p}, \frac{\Delta\Omega_1/2 + \delta\Omega_{\rm prec}}{\pi}\frac{\Delta\Omega_1/2}{\dot{\Omega}P_p}] \\ \quad \text{if } \pi/2 - f_2 > \mathrm{asin}(a_{b,1}/a_p) \\ \quad \& \ \Delta\Omega_1/2 + \delta\Omega_{\rm prec} > \pi \\ \min[\frac{T_{\rm obs}}{P_p}, \frac{\Delta\Omega_1/2}{\dot{\Omega}P_p}], \\ \quad \text{else if } \pi/2 - f_2 > \mathrm{asin}(a_{b,1}/a_p) \\ \min[\frac{T_{\rm obs}}{P_p}, \frac{\Delta\Omega_1 + \delta\Omega_{\rm prec}}{2\pi}\frac{\Delta\Omega_1}{\dot{\Omega}P_p}] \\ \quad \text{else if } \Delta\Omega_1 + \delta\Omega_{\rm prec} > 2\pi \\ \min[\frac{T_{\rm obs}}{P_p}, \frac{\Delta\Omega_1}{\dot{\Omega}P_p}] \\ \quad \text{else.} \end{cases} \quad (18)$$

Assuming each orbit crossing is independent, the probability to transit the star m_1 at least once is:

$$P_{\rm cr,1}(1 - (1 - P_{*,1})^{n_1}). \quad (19)$$

Equation (19) can be applied to systems involving a faint star, where only the transit of the primary star can be detected.

Considering transits of both stars, one can obtain the probability for the planet to transit the two stars at least once:

$$P_{\rm transit} = P_{\rm cr,2}\left[1 - (1 - P_{*,2})^{n_2}\left(\frac{P_{\rm cr,1}}{P_{\rm cr,2}}(1 - P_{*,1})^{n_1} + \frac{P_{\rm cr,2} - P_{\rm cr,1}}{P_{\rm cr,2}}\right)\right] \quad (20)$$

where $m_1 > m_2$, because if a planet crosses the orbit of m_2, it can also cross the orbit of m_1. For simplicity, we assume that, if the planet crosses both stellar orbits, the transit events are independent. Note that the independence approximation does not generally hold, because the stars are 180° out of phase with each other, and each orbit crossing has a roughly fixed phase difference between each other, due to the periodic nature of the stellar orbits. However, we illustrate in the following section (Section 3.2) that the transit probability obtained using the independence approximation agrees well with the numerical results.

In addition, one can also calculate the average number of transits given that a system transits. The average number of transits can help determine the likelihood to detect the transit events, since it's more likely to detect the planet when the transit number increases. Specifically, the averaged number of transits can be expressed as the following:

$$N_{\rm transit} = n_2 P_{*,2} + n_1 P_{*,1} P_{\rm cr,1}/P_{\rm cr,2}, \quad (21)$$

Here, similar to Equation (20), we assume $m_1 > m_2$. As shown in the following Section 3.2, the analytical expression agrees with the numerical results—except at low mutual inclination, where the independence approximation causes the averaged number of transits to be larger than the numerical results. Specifically, the expected number of transits differ within a factor of two (see more discussions in section Section 3.2).

3.2. Numerical Comparison

To test how well the analytical expression predicts the transit probability, we compare the analytical results with the numerical transit probabilities obtained from numerical simulations. We include three sets of planetary systems for illustration: planetary systems with equal-mass stellar binaries with line-of-sight inclination at 90° (Section 3.2.1), planetary systems with eclipsing equal-mass stellar binaries (i_b near—but not exactly—90°; cf., Section 3.2.2), and the observed planetary systems with un-equal mass stellar binaries in eccentric orbits around eclipsing binaries (Section 3.2.3).

3.2.1. Equal-mass Stellar Binaries Along Line-of-Sight

In this section, we consider the transit probability for planetary systems composed of two solar-type stars in a circular orbit, surrounded by planets with different semimajor axes and mutual inclinations. The transit probability depends sensitively on the mutual inclination between the stellar orbit and the planetary orbit. Thus, we first check the analytical results against numerical results that include different mutual inclinations. In this section, we set the stellar binary to be aligned with the line-of-sight first; we relax this assumption in the next section (Section 3.2.2). Specifically, for each mutual inclination, we run 1000 numerical simulations with planetary true anomaly (f) and longitude of ascending node (Ω) randomly drawn from a uniform distribution. We record the number of systems in which the planet transits in front of the stars to obtain the transit probability for each mutual inclination.

The upper panel of Figure 3 shows the probability that either of the binary stars will transit at least once in one year, when the orbital period of the stellar binaries is two days; the lower panel shows the case when the orbital period is five days. The solid lines represent the results of the analytical expression we derived in Section 3.1 (see Equation (20)), and the crosses are

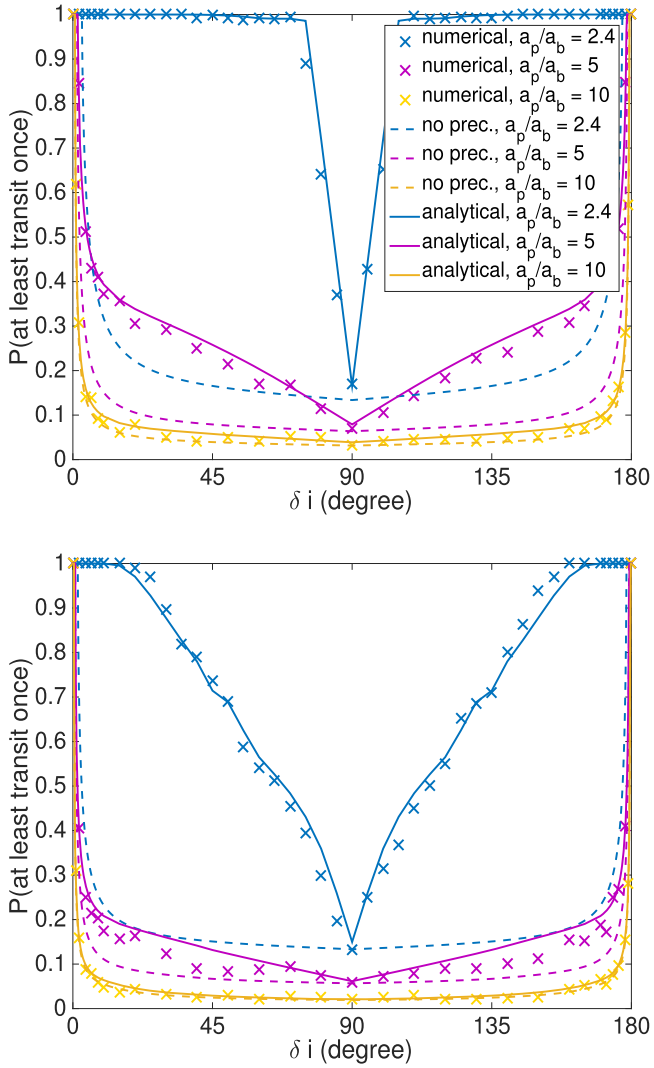

Figure 3. Upper panel: transit probability in one year for circumbinary planets surrounding a $P = 2$ day stellar binary, as a function of δi. Lower panel: transit probability for planets surrounding a $P = 5$ day stellar binary, as a function of δi. The solid lines indicate the analytical results, and the crosses are the numerical results. The dashed lines represent the case without precession. The analytical results agree well with the numerical simulation, and the transit probability is greatly under-predicted without precession.

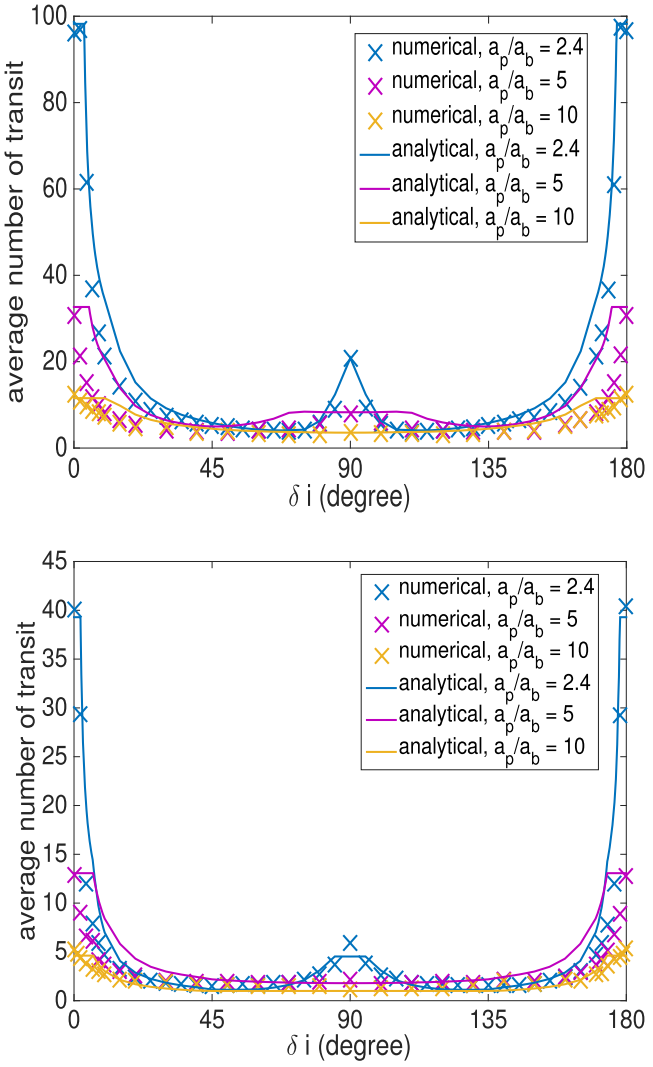

Figure 4. Upper panel: average number of transits, given that the system transits at least once, surrounding a $P = 2$-day stellar binary, as a function of δi; lower panel: average number of transits, given that the system transits at least once, surrounding a $P = 5$-day stellar binary, as a function of δi. The analytical expression over-estimates the number of transit within a factor of two, at low mutual inclinations.

the numerical results. The different colors represent the different planet-to-stellar semimajor axis ratios. The blue crosses represent the probability when the planetary semimajor axis is 2.4 times that of the stellar binary, where the critical semimajor axis for stability is $\sim 2.4 a_b$ in these cases, according to the stability limit by Equation (1) (Holman & Wiegert 1999). The purple crosses represent the case when $a_p/a_b = 5$, and the yellow crosses represent the case when $a_p/a_b = 10$. For all the cases included here, the analytical results agree very well with the numerical results. In addition, different from the case with an infinite amount of observation time, where Martin & Triaud (2015) found that the transit probability increases as the mutual inclination increases, the transit probability decreases as the mutual inclination increases in the finite observation time case, when $i_b = 90°$.

The dashed lines in Figure 3 represent the case when we ignore orbital precession. At low mutual inclinations, the precession timescale is shorter, and the parameter space that allows transit increases. Therefore, at lower mutual inclinations, the transit probability is much higher when one includes orbital precession. This agrees with Martin & Triaud (2015). At $\sim 90°$, the precession time is long, and the results with and without orbit precession become similar. Moreover, the precession timescale increases steeply with the planetary orbital period. Thus, when the semimajor axis of the planet is larger, the difference between the cases with and without precession also becomes smaller.

The number of transits is important for planet detection, because the more the planet transits the stars, the more likely it can be detected. For instance, all detected circumbinary systems have had at least three primary and/or secondary transits upon publication. To investigate this, we record the number of transits for each system in the simulation, to obtain the average number of transits for each mutual inclination—given that the planet transits at least once. The results are shown in Figure 4. Similar to Figure 3, the upper panel shows the case when the planet orbits a circular two-day stellar binary

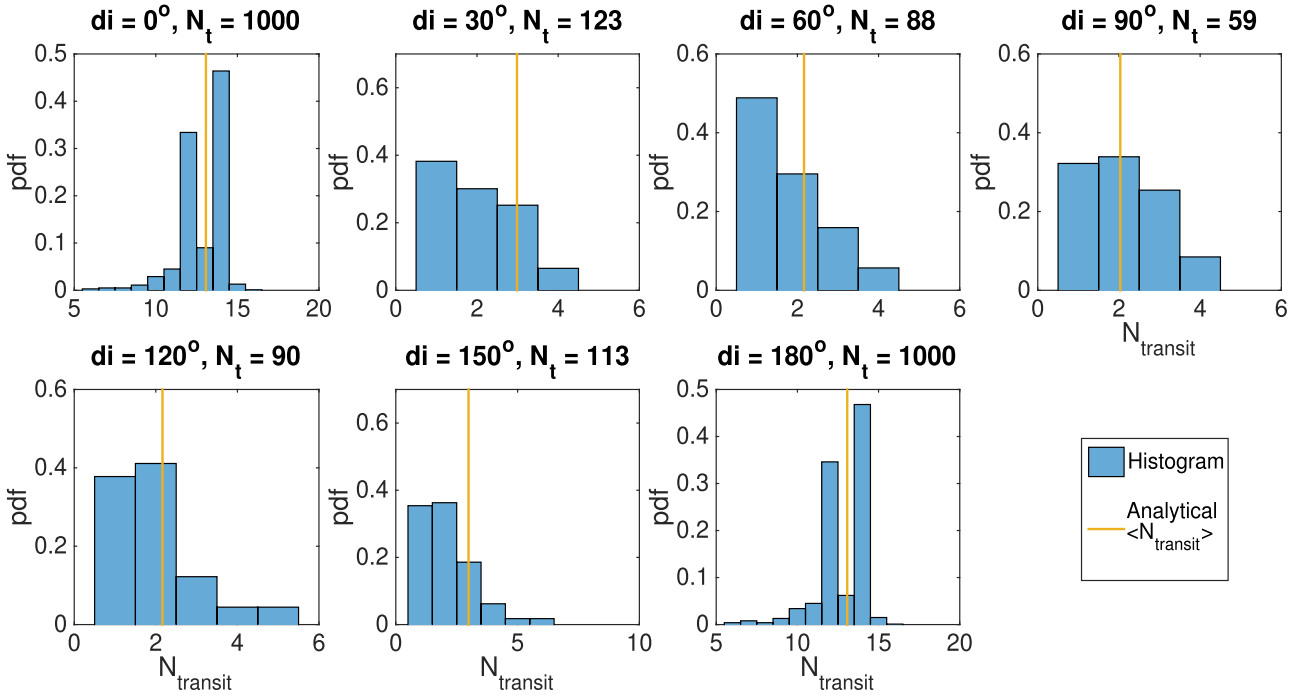

Figure 5. Distribution of the number of transits in one year. The planetary semimajor axis is set to be five times that of the stellar binary ($a_p/a_b = 5$), and the stellar binary period is five days $P_* = 5$ days. Each panel corresponds to a different mutual inclination, and the number of systems that transit at least once is shown in the title of each panel.

with solar masses and solar radii, and the lower panel shows the case when the planet orbits a circular five-day stellar binary. We also include planets with three different semimajor axes ($a_p = 2.4a_b$, $a_p = 5a_b$, and $a_p = 10a_b$) represented by different colors. As expected, the average number of transits is smaller when the planetary orbit is farther from the stellar binary—where the range of node longitude that allows transits is smaller, and the orbital period is longer. Interestingly, the average number of transits is larger when the mutual inclination is around $\sim 90°$. This is because the precession time is long when the mutual inclination is higher, and the longitude of node will stay longer in the range that allows transits, which leads to a higher average number of transits for planetary systems that transit at least once.

Comparing the analytical results (solid lines; Equation 21) with the numerical results (crosses), Figure 4 shows that, at low mutual inclinations, the analytical expression systematically leads to a larger average number of transits than the numerical results. This is because the transit events of the two stars are not independent, as assumed in the analytical derivation. Because the two stars are 180° out of phase with each other, the likelihood for both of the stars to transit is reduced. This reduction is important when the mutual inclination is lower, where $P_{*,1\ or\ 2}$ is so large that the likelihood for the two stars to both transit is high—assuming that the transits are independent. Because the reduction may change a double transit to a single transit during one planetary orbit period, it can, at most, decrease the average number by a factor of two. Thus, as shown in Figure 4, the average number of transits from the analytical expression is consistent, within a factor of two, with the numerical results.

To illustrate the distribution of the number of transits, Figure 5 shows the histogram of the number of transits for the circumbinary planetary systems with a five-day stellar orbit, and a planet-to-stellar semimajor axis ratio of five. Each panel corresponds to a different mutual inclination (δi), and we include 1000 systems with random orbital phases to obtain the results in the histogram. The widths of the bins are unity, and the number of systems that transit at least once (N_t) is shown in the title of each panel. The yellow solid line represents the average number according to the analytical expression (see Equation (21)).

The results in Figure 5 can be understood from geometrical interpretations. Specific to this case, the planet period is roughly 56 days; in one year, the planet orbits 6.5 times. Thus, the maximum number of transits is $2 \times (6 + 2) = 16$ times, where the planet transits both stars before and after the full orbits, agreeing with the numerical results shown in Figure 5. When the mutual inclination is low $\sim 0°$, the planet transits the stars every orbit. Because the stars may overlap in projection during the transit, the minimum number of transits is six. Moreover, the average number of transits peaks around $2 \times 6 = 12$ and $2 \times 7 = 14$ times, when the mutual inclination is 0 or 180°, as shown in Figure 5. At high mutual inclinations, the histograms show that the planet still has a high probability to transit at least twice; thus, it is unlikely to miss the transits. The average number of transits is symmetric with respect to 90°, and the deviation from this symmetry is due to the random fluctuations.

3.2.2. Eclipsing Equal-mass Stellar Binaries

Because the stellar binaries do not need to be aligned at $i_b = 90°$ in order to eclipse, we also consider the case when i_b near—but not exactly—90°. This is very different from the case when $i_b = 90°$, especially for low δi. Specifically, the planet cannot transit the stars when the mutual inclination $\delta i < i_{p,c,1} = |\Delta i_b| - \mathrm{asin}[(a_{b,1} \sin \Delta i_b + R_{*,1})/a_p]$, where

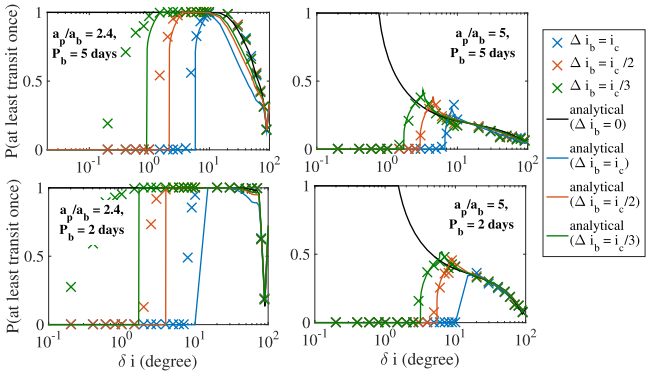

Figure 6. Probability that a planet transits at least once in one year, as a function of δi, when $a_p = 2.4a_b$ (left panels) and when $a_p = 5a_b$ (right panel). The crosses represent the numerical results, and the solid lines represent the analytical results. The analytical expression does not fit well when $a_p = 2.4a_b$, because the planetary orbit is no longer circular due to the strong perturbation of the stellar binary.

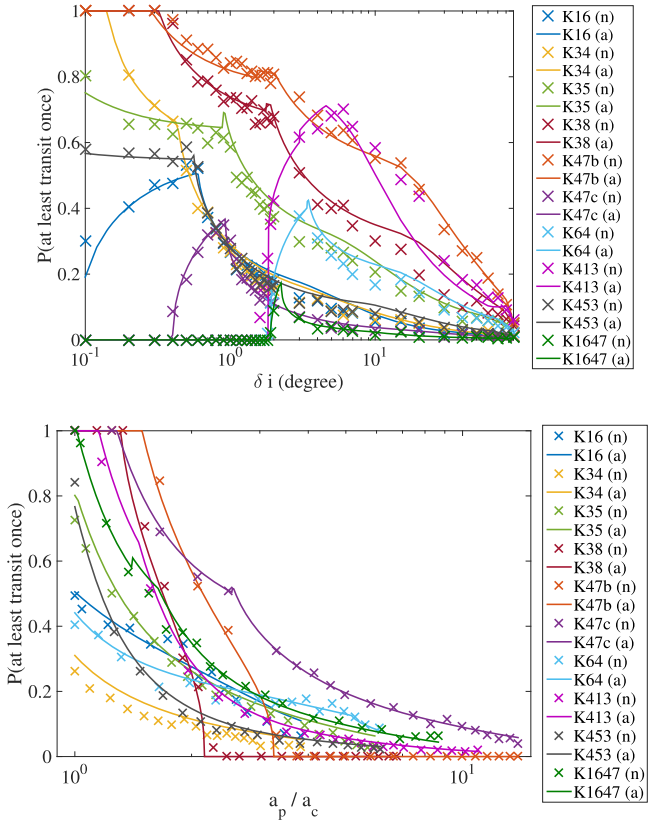

Figure 7. Probability that a planet transits at least once during the observation interval, as a function of δi (upper panel) and a_p/a_c (lower panel) for the observed transiting systems. The crosses represent the numerical results, and the solid lines represent the analytical results. The analytical results agree quite well with the numerical results.

$\Delta i_b = 90 - i_b^\circ$, as mentioned in Section 3.1. Considering the transit of both stars, $P_{\rm transit} = 0$ when $\delta i < \min[i_{p,c,1}, i_{p,c,2}]$.

To compare the analytical expression of the transit probability with numerical results, we set the binary star to be Sun-like, in a circular orbit, with orbital periods of two and five days; we simulate the case when the planet semimajor axis is set to be $a_p = 2.4a_b$ and $a_p = 5a_b$, similar to Section 3.2.1. The critical line-of-sight inclination for the stellar binary to eclipse is $i_c = 2\,R_\odot/a_b = 13\overset{\circ}{.}7$ when the stellar binary is in a two-day orbit, and $i_c = 2R_\odot/a_b = 7\overset{\circ}{.}4$ when the stellar binary is in a five-day orbit. To include different stellar inclinations, we set $i_b = i_c$, $i_b = i_c/2$ and $i_b = i_c/3$ separately. The results are shown in Figure 6.

Figure 6 shows the transit probability over one year. The numerical results are indicated by crosses, and the analytical results are represented by the solid lines. Note that, when $a_p/a_b = 2.4$, the planet can still transit when δi is smaller than the critical value. This is because the minimum separation $r_{p,\rm min}$ is smaller than the semimajor axis of the planet, a_p, because the planetary orbit is not circular and the semimajor axis can vary from its initial value due to the perturbation of the stellar binary. Thus, the analytical results do not agree well with the numerical results when $a_p/a_b = 2.4$. The discrepancy is smaller when $|\Delta_{ib}|$ is smaller. In addition, Figure 6 shows that, when δi is large, the transit probability approaches the results when i_b is set to be 90°.

It was found by Martin & Triaud (2015) that, given an infinite amount of time, the transit probability of circumbinary planets is higher than that of planets orbiting a single star. However, this is not always true for a finite observation time, especially when the total observation time is very short. For instance, the precession of the planetary orbit is faster for the circumbinary planets, and allows a larger parameter space for the planet to cross the stellar orbit—yet the planet may not transit the star when it crosses the binary orbit. Specifically, the probability to transit a single star is $P = R_*/a_p$ for a circular planetary orbit (Borucki & Summers 1984). For planets around a five-day orbital period stellar binary at $a_p/a_b = 2.4$, the one-month transit probability of the circumbinary planets is higher than the case where we substitute the stellar binary with a single solar-type star, where the probability to transit is $P = R_\odot/a_p = 0.027$. However, at $a_p/a_b = 5$, the transit probability of the circumbinary planets in one month is lower than that orbiting a single solar-type star when the mutual inclination between the planet and the binary star is high ($\gtrsim$50°). When the total observation time is increased to $\gtrsim$60 days, the probability to transit is lower for the single-star case, even at $a_p/a_b = 5$ for all δi. This suggests that, for the *TESS* mission, some of the circumbinary planets may have lower transit probabilities than those of their counterpart planets around single stars.

3.2.3. Observed Circumbinary Planets

To test the analytical expression when the stellar binaries are composed of stars with different stellar masses and in eccentric stellar orbits, we numerically obtain the transit probability for the observed circumbinary planets, and compare the analytical results with the numerical simulation. In this section, we allow the stellar inclination $i_b \neq 90°$. The properties of the circumbinary planets are listed in Table 1. Most of the planetary orbits are nearly circular, except Kepler-47c. However, the eccentricity of Kepler-47c is quite uncertain. Thus, for simplicity, we set the planetary orbits to be circular.

Note that Hinse et al. (2015) studied the possibility of a third circumbinary planet in Kepler-47, based on a single transiting event, and put an upper limit in the semimajor axis of the third planet by analyzing the transit duration. We exclude the third planet in our calculations, because the orbital parameters of this object are still largely uncertain.

For each planetary system, we use the observed properties listed in Table 1, and vary the mutual inclination between the

Table 1
Properties of Observed Transiting Circumbinary Planets

	$m_1(M_\odot)$	$m_2(M_\odot)$	$R_{*,1}(R_\odot)$	$R_{*,2}(R_\odot)$	a_b(au)	e_b	$m_p(M_J)$	$R_p(R_J)$	a_p(au)	δi(°)	e_p	i_b(°)
Kepler 16b[a]	0.69	0.20	0.65	0.23	0.22	0.16	0.33	0.75	0.70	0.31	0.0069	90.34
Kepler 34b[b]	1.05	1.02	1.16	1.09	0.23	0.52	0.22	0.76	1.09	1.86	0.18	89.86
Kepler 35b[c]	0.89	0.81	1.03	0.79	0.18	0.14	0.13	0.73	0.60	1.07	0.042	90.42
Kepler 38b[d]	0.95	0.25	1.76	0.27	0.15	0.10	<0.38	0.39	0.46	0.18	<0.032	89.27
Kepler 47b[e]	1.04	0.36	0.96	0.35	0.084	0.023	0.022–0.031	0.27	0.30	0.27	<0.035	89.34
Kepler 47c[f]	1.04	0.36	0.96	0.35	0.084	0.023	0.050–0.072	0.42	0.99	1.16	<0.41	89.34
Kepler 64b[g]	1.53	0.41	1.73	0.38	0.17	0.21	<0.531	0.56	0.63	2.81	0.054	87.36
Kepler 413b[h]	0.82	0.54	0.78	0.48	0.10	0.037	0.21	0.40	0.36	4.07	0.12	87.59
Kepler 453b[i]	0.93	0.19	0.83	0.21	0.18	0.051	0.00031	0.56	0.79	2.30	0.038	90.28
Kepler-1647b[j]	1.22	0.97	1.79	0.97	0.13	0.16	1.52	1.08	2.72	2.99	0.058	87.92

Notes.
[a] Data obtained from Table 1 of Doyle et al. (2011). Here, a_p differs from Martin & Triaud (2015), who set $a_p = 0.71$ au, and δi is obtained from Table 1 of Martin & Triaud (2015).
[b] Data obtained from Table 1 of Welsh et al. (2012). Here, $R_{*,2}$ differs from Martin & Triaud (2015), who had a typo and set $R_{*,2} = 0.19\,R_\odot$ in their Table 1; δi is also obtained from Table 1 of Martin & Triaud (2015).
[c] Data obtained from Table 1 of Welsh et al. (2012), with δi obtained from Table 1 of Martin & Triaud (2015).
[d] Data obtained from Table 6 of Orosz et al. (2012a), where m_2 and $R_{*,1}$ differ from Martin & Triaud (2015), who set them to be $0.27\,M_\odot$ and $1.78\,R_\odot$ separately. In the numerical simulation, m_p is set to be $0.38\,M_J$. The results are not sensitive to the planetary mass, because $m_p \ll m_{1,2}$.
[e] Data obtained from Table 1 and the main text of Orosz et al. (2012b). We adopt $m_p = 0.031\,M_J$ for numerical simulation. The results are not sensitive to the planetary mass, because $m_p \ll m_{1,2}$. Our m_2, $R_{*,1}$, and $R_{*,2}$ differ from Martin & Triaud (2015), who set m_2 to be $0.46\,M_\odot$, $R_{*,1}$ to be $0.84\,R_\odot$, and $R_{*,2}$ to be $0.36\,R_\odot$.
[f] Same as K-47b, we obtain data from Orosz et al. (2012b). We set $m_p = 0.072\,M_J$ for numerical simulation. The results are not sensitive to the planetary mass, because $m_p \ll m_{1,2}$.
[g] Schwamb et al. (2013) and Kostov et al. (2013). The results of both studies are consistent with each other. For the simulations, we use the results of Schwamb et al. (2013), and set $m_p = 0.531 M_J$ in the numerical simulation. Our $m_{*,1}$, $m_{*,2}$, $R_{*,1}$, $R_{*,2}$, a_b, and a_p all differ from Martin & Triaud (2015), who set $m_{*,1} = 1.50$, $m_{*,2} = 0.40$, $R_{*,1} = 1.75$, $R_{*,2} = 0.42$, $a_b = 0.18$, and $a_p = 0.65$.
[h] Data obtained from Table 4 of Kostov et al. (2014). Our $m_{*,2}$ and δi differ from Martin & Triaud (2015), who set $m_{*,2} = 0.52\,M_\odot$ and $\delta i = 4.^\circ 02$.
[i] Data obtained from Table 3 of Welsh et al. (2015). Note that m_p is highly uncertain, because $m_p = 0.00031 \pm 0.050 M_J$. Our a_p differs from Martin & Triaud (2015), who set it to be 0.93 AU.
[j] Data obtained from Table 4 of Kostov et al. (2015).

planetary and stellar orbits—or the planetary semimajor axis—to obtain the transit probability, as a function of the mutual inclination or the planetary semimajor axis. We then compare the analytical and numerical results for different mutual inclinations and planetary orbital semimajor axes.

The detection periods for the different systems vary. According to the discovery papers (Doyle et al. 2011; Orosz et al. 2012a, 2012b; Welsh et al. 2012, 2015; Kostov et al. 2013, 2014; Schwamb et al. 2013; Kostov et al. 2015), the circumbinary systems are detected using different number of *Kepler* observation quarters; thus, the transits occur in different total time intervals. Therefore, we set the integration time to be 600, 671, 671, 967, 1050.51, 967, 1340, 1470, and 1470 days, respectively, for Kepler-16, Kepler-34, Kepler-35, Kepler-38, Kepler-47, Kepler-64, Kepler-413, Kepler-453, and Kepler-1647, in the numerical simulations, as shown in Table 2. In addition, the secondary stars are very faint in Kepler-38, Kepler-47, Kepler-64, Kepler-413, and Kepler-453, where only the transit of the primary star is detectable. Thus, in the numerical simulations, we only take into account the transits of the primary stars for these systems.

The upper panel of Figure 10 shows the probability to transit both of the stars or the primary star during the different observation interval, as summarized in the paragraph above. We vary the mutual inclination ranges from 0° to 180°. The crosses represent the results from numerical simulations, and the solid lines represent the analytical results. It is shown that the analytical results are consistent with the numerical results for the cases considering the transit of both stars as well as the transit of only the primary stars. The planet still has a high probability to transit when the mutual inclination reaches ∼5°. Note that, at high inclinations, the ascending node librates; this may introduce a discrepancy between the numerical results and the analytical results, as discussed by Martin & Triaud (2015). In addition, planets with higher mutual inclination (∼1°–3°) may be more likely to transit, for systems with large $|\Delta i_b|$, as pointed out by Martin & Triaud (2015).

The lower panel of Figure 10 shows the probability to transit at least once in the observational interval, as a function of the planetary semimajor axis to the stability ratio. We set the minimum planetary semimajor axis to be the critical semimajor axis, beyond which the planet is stable (from Equation 1) and we set the maximum semimajor axis to be that corresponding to a four year orbit. Overall, the analytical results (solid lines) are also consistent with the numerical results (crosses). The numerical probability are used in Section 4 to derive many properties of the architecture of the circumbinaries.

Table 2
Integration Time (Days) of the Observed Transiting Circumbinary Planets

Kepler 16	Kepler-34	Kepler-35	Kepler-38	Kepler-47
600	671	671	967	1050.51
Kepler-64	Kepler-413	Kepler-453	Kepler-1647	
967	1340	1470	1470	

4. CIRCUMBINARY PLANETARY ARCHITECTURE

The architectures of the circumbinary planetary systems provide important clues on the formation of planetary systems. In this section, we focus on the observed transiting circumbinary systems and study their orbital properties. To accurately determine the role of selection bias, we use the transit probability directly from numerical integrations. Note that, in addition to transits, another indicator of circumbinary planets is a variation in the eclipse timings (ETVs). This is noticeable in roughly half of the *Kepler* sample, and may introduce a detection bias that we have not considered. This approach differs from Armstrong et al. (2014) and Martin & Triaud (2014), who studied the abundance of circumbinary planetary systems using population synthesis.

4.1. Distribution of a_p

It has been found that most of the innermost transiting circumbinary planets reside near the stability limit, close to the stellar binary (Armstrong et al. 2014). This may indicate the dominance of migration during planet formation. However, this may also be due to selection effects, because close-in planets admit larger orbital parameter spaces which allow transits, and thus are more likely to be detected. Using population synthesis, Martin & Triaud (2014) found that selection biases alone cannot account for the pile-up near the stability limit. Recently, Kepler-1647 was discovered to orbit far from the stability limit (Kostov et al. 2015). In this section, we consider multiple semimajor axis distributions, and include the newly discovered Kepler-1647 to study the pile-up of planets near the stability limit, using a Bayesian approach to take the selection bias into account.

To take selection effects into account, we require planets to transit at least twice to be detected. We then study the significance of the pile-up, using a hypothesis test. Specifically, our null hypothesis is that the distribution of the detected planetary semimajor axis follows the conditional probability distribution of the semimajor axis, given that the planets transit at least twice ($P(\tilde{a}_p|tt_2)$), where tt_2 stands for the event that a planet transits at least twice. Next, we calculate the probability that the planetary semimajor axis is smaller than the observed value. If this probability is very small, it rejects the null hypothesis and indicates that the reason the planet locates near the stability limit is not due only to selection effects. Using the Bayesian approach, $P(\tilde{a}_p|tt_2)$ ($\tilde{a}_p = a_p/a_c$) can be expressed as the following:

$$P(\tilde{a}_p|tt_2) = \frac{P(tt_2|\tilde{a}_p)P(\tilde{a}_p)}{\int_{(\tilde{a}_p)_{\min}}^{(\tilde{a}_p)_{\max}} P(tt_2|a')P(a')\,da'}, \quad (22)$$

where $\tilde{a}_{p,\min} = 1$ for stability purposes, and $\tilde{a}_{p,\max}$ corresponds to orbital periods equal to the total time of detection obtained from the discovery papers, as summarized in the beginning of this section.

Here, $P(tt_2|\tilde{a}_p)$ stands for the probability to transit at least twice across different planetary semimajor axes, $\tilde{a}_p$. This probability can be obtained using the analytical expression or numerical simulations, as described in the previous section. We use the numerical values directly for the following analysis. Here, $P(\tilde{a}_p)$ is the prior of $\tilde{a}_p$, and we assume a uniform distribution for the following reasons. First, the signal-to-noise level is important in the detection of the circumbinary planets.

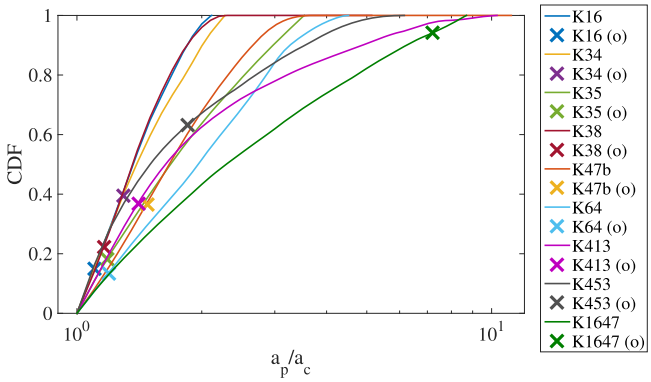

Figure 8. Cumulative distribution function of the scaled semimajor axis ($\tilde{a}_p = a_p/a_c$), given that the planet transit at least twice. The crosses represent the observed value of the innermost planets for each system. Except for Kepler-1647b and Kepler-453b, the probability that the scaled semimajor is smaller than the observed value is $\lesssim$50%.

In particular, the signal-to-noise level (S/N) of the transit depends on the distance between the planet and the stellar binary:

$$s/n \propto \sqrt{n_{\rm tr} t_{\rm dur}}. \quad (23)$$

Here, $n_{\rm tr}$ stands for the number of transits, and $t_{\rm dur}$ is the transit duration time. The transits of the same circumbinary system can be very different, depending on the relative velocity between the star and the planet during the transits. Thus, each transit needs to be resolved separately. Therefore, $s/n \propto \sqrt{t_{\rm dur}}$. The explicit expression for the transit has been derived by Kostov et al. (2014), where the dependence on a_p is weak, and the duration time increases when the planet-star distance increases—assuming the impact parameter is independent of a_p, because the dependence of the impact parameter on a_p is not trivial, especially when $\Delta_{ib} \neq 0$. Thus, it is easier to detect the planet when it is farther away, in terms of S/N level. To obtain the lower limit constraint (maximum value of $P(\tilde{a}_p < \tilde{a}_{p,\rm obs}|tt_2)$) on the pile-up near the stability limit, we use a uniform prior where $P(\tilde{a}_p) = 1/((\tilde{a}_p)_{\max} - (\tilde{a}_p)_{\min})$. Second, note that Armstrong et al. (2014) simulated the recovery rate of transit detection for circumbinary systems, and showed that the recovery rate decreases mildly with orbital period, based on simulations with $P_p = 10.2P_b$ and $P_p = 300$ days. However, a detailed scaling was not included. The decrease of the detection probability as a function of planetary distance may be inherited in the detection algorithm, where a larger number of the transits makes it less likely to miss the transits. Because the recovery rate only decreases mildly, and no detailed scaling as a function of a_p is available yet, we do not take this into account here.

The cumulative distribution of $\tilde{a}_p$, given that the planet transits twice, for the observed innermost planet is shown in Figure 8. The crosses represent the observed results. Except for the newly discovered Kepler-453b and Kepler-1647b, which have a large probability that $\tilde{a}_p$ is smaller than the observed value, most of the planets are moderately close to the stability limit—with probability $\lesssim$40%. However, these probabilities are not small enough to reject the null hypothesis.

Because most of the innermost planets (except Kepler-1647b) have $P(\tilde{a}_p < \tilde{a}_{p,\rm obs}|tt_2) < 50\%$, the collective feature

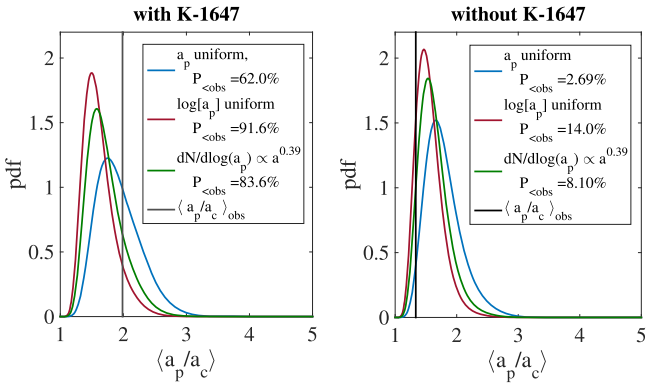

Figure 9. Probability distribution function of the mean of a_p/a_c, for the innermost planets in the observed transiting systems. The left panel represents the case with Kepler-1647b, and the right panel represent the case without Kepler-1647b. The solid black lines indicate the observed values. The different colored lines represent the case with different prior distribution. Excluding Kepler-1647b, the probability that a_p/a_c is smaller than the observed value is very small, indicating that the pile-up near the stability limit is not due to selection effect—if the prior is uniform in a_p/a_c.

of these systems may suggest that there exists a pile-up near the stability limit. To investigate their collective behavior, we designed a numerical hypothesis test. Specifically, we take all the observed transiting circumbinary systems together, and use the averaged $\tilde{a}_p$ ($\langle\tilde{a}_p\rangle$) as a statistic to test the null hypothesis that $\tilde{a}_p$ follows $P(\tilde{a}_p|tt_2)$ according to Equation (22) for each system. Specifically, if, under the null hypothesis, the observed $\langle\tilde{a}_p\rangle$ or the values smaller than that have a very small probability (<5%), we reject the null hypothesis, and we claim that there is likely a pile-up of planets near the stability, after taking into account selection effects.

We numerically convolve the distribution of $\tilde{a}_p$ for all the systems, in order to obtain the distribution of $\langle\tilde{a}_p\rangle$, and the result is represented by the blue lines in Figure 9. Excluding Kepler-1647, the probability that the averaged $\tilde{a}_p$ is smaller than the observed value is very small (2.69%), suggesting that there is likely a pile-up after considering the selection effects. This is consistent with the population synthesis study by Martin & Triaud (2014). However, including Kepler-1647, the probability is much larger (reaching ∼62%) indicating that the null hypothesis cannot be rejected. There are two possibilities: if Kepler-1647 shares the same distribution as the other nine systems, there is likely no pile-up of planets near the stability limit; if Kepler-1647 is an outlier of this sample, which follows a different semimajor axis distribution, then there is likely a pile-up for some population of the circumbinary planetary systems. More observations of the transiting circumbinary systems can help distinguish this. Note that the probability only differs within a factor of two, if we take transits of both stars into account and integrate over four years for all the observed systems.

The distribution of planetary periods for single star systems has been studied in the literature (Winn & Fabrycky 2015). For instance, for smaller-sized planets (1–4$R_\oplus$) with a period range of 20–200 days, Silburt et al. (2015) have found that the planetary period follows a log-uniform distribution, where $dN/da_p \sim \propto a_p^{-1}$, consistent with Youdin 2011; Howard et al. 2012; Fressin et al. 2013; and Petigura et al. 2013. For larger-sized planets (4–8$R_\oplus$), the probability density can be expressed as $dN/d\log P_p \propto P_p^{0.7}$ (Dong & Zhu 2013), where the semimajor axis distribution is nearly uniform $dN/da_p \sim \propto a_p^{0}$. From radio velocity studies, Cumming et al. (2008) obtained that $dN/d\log P_p \propto P_p^{0.26}$, where $dN/da_p \sim \propto a_p^{-0.61}$ for planet mass >0.4M_J, and orbital period <2000 days. Next, we check whether the circumbinary planetary systems may follow distributions to the planets around single stars, and whether this, in addition to the selection effect, can explain the observed pile-up.

Using a log-uniform distribution as a prior, the results on the probability density function of $\langle\tilde{a}_p\rangle$ are shown by the red lines in Figure 9. Excluding Kepler-1647, the probability that $\langle\tilde{a}_p\rangle$ is smaller than the observed value is 14%; including Kepler-1647, the probability that $\langle\tilde{a}_p\rangle$ is smaller than the observed value 91.6%. Both cases cannot rule out the hypothesis that the planetary period follows a log-uniform distribution, suggesting that there is no additional pile-up if the circumbinary planets share the log-uniform period distribution, because the smaller-sized planets orbit single stars. The green lines in Figure 9 show the case when the prior follows $dN/d\tilde{a}_p \sim \propto \tilde{a}_p^{-0.61}$. The probability that $\langle\tilde{a}_p\rangle$ is smaller than the observed value is 8.1%, excluding Kepler-1647, and is 83.6% including Kepler-1647. Neither of the cases rule out the hypothesis that the circumbinary planetary system follows a distribution ($dN/d\log P_p \propto P_p^{0.26}$) similar to the planets around single stars, obtained from the RV measurements by Cumming et al. (2008). This also suggests that the pile-up is consistent with this period distribution and these selection effects. On the other hand, the circumbinary planets do not favor the period distribution of larger planets around single stars ($dN/d\log P_p \propto P_p^{0.7}$), obtained by Dong & Zhu (2013), where selection effects alone cannot explain the pile-up near the stability limit.

4.2. Coplanarity

The observed transiting circumbinary planets all have small mutual inclinations between their planetary orbits and the stellar binary (as shown in Table 1). This may be primordial, because the observed circumbinary protoplanetary disks are also aligned with the stellar orbit within ∼3° (e.g., Czekala et al. 2016). However, this may also be due to selection effects, because systems with near-coplanar configurations are more likely to be observed via the transit method. To test whether the coplanarity is only a selection effect, and to put a constraint on the mutual inclination distribution, we identify the probability distribution of the mutual inclination that is consistent with the observations, while taking into account the selection bias.

Similar to our study on the distribution of planetary semimajor axes in the previous section, we require the planet to transit at least twice for a robust detection, and our null hypothesis is that the distribution of the observed mutual inclination follows the conditional probability distribution, given that the planet transits at least twice ($P(\delta i|tt_2)$), where δi is the mutual inclination, and tt_2 represents the event that a planet transits at least twice. If the probability of that the mutual inclination being smaller than the observed value is <5% (i.e., very small), it rejects the null hypothesis and it indicates that the mutual inclination follows a distribution with a smaller spread than the prior. Specifically,

$$P(\delta i|tt_2) = \frac{P(tt_2|\delta i)P(\delta i)}{\int_{i'=0}^{i'=180} P(tt_2|\delta i = i')P(\delta i = i')di'}, \quad (24)$$

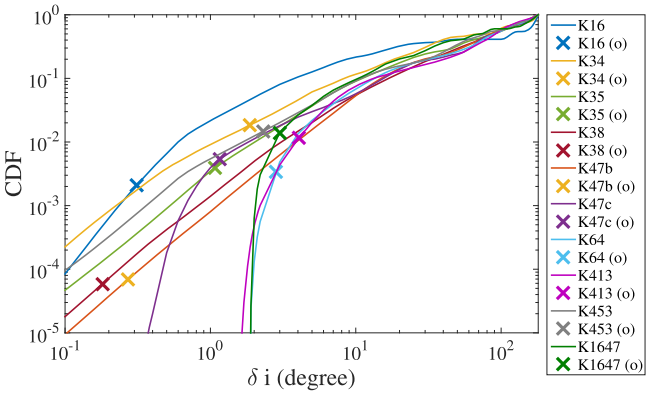

Figure 10. Probability of the mutual inclination, given that the planet transits at least twice, assuming the prior distribution of δi is isotropic. The crosses represent the observed value. The probability that the mutual inclination is smaller than the observed value is very small, indicating that the mutual inclination is likely small.

where $P(tt_2|\delta i)$ can be obtained from the analytical approach. In the following analysis, we directly use results from the numerical simulations described in Section 3.2.3.

Assuming an isotropic distribution as the prior ($P(\delta i) = \sin i/2$), the cumulative distribution of $P(\delta i|tt_2)$ is shown in Figure 10, where the crosses represent the observed mutual inclination. It shows that the probability that the mutual inclination is smaller than the observed value is very small ($\lesssim$1%). Thus, it is highly unlikely that the observed coplanarity of the systems is only due to selection effects. This suggests that the observed circumbinary planets are likely formed near the orbital plane of the stellar binary.

We next use different prior distributions to further investigate the distribution of the mutual inclination. We assume that the prior of the mutual inclination follows a Fisher distribution ($f(\delta i|\kappa)$), also known as a $p = 3$ von Mises–Fisher distribution, which is a probability distribution of the two-dimensional sphere in three-dimensional space. This is similar to the model of the spin–orbit misalignment distribution discussed in the literature (e.g., Fabrycky & Winn 2009; Li & Winn 2016). Specifically,

$$f_\kappa(\delta i) = \frac{\kappa}{2\sinh\kappa} e^{\kappa\cos\delta i}\sin\delta i, \quad (25)$$

where the concentration parameter κ controls the spread in mutual inclination. For large κ, $f_\kappa(\delta i)$ approaches Rayleigh distribution with width $\sigma \to \kappa^{-1/2}$. When $\kappa \to 0$, the distribution is isotropic.

For large κ, the prior distribution of the inclination concentrates in the near co-planar regime, and the probability of the mutual inclination to be smaller than the observed values may be $\lesssim$50% for many of the observed systems. In such cases, the collective behavior of the observed systems may still indicate a narrower spread. Therefore, similar to our study on the semimajor axis, we design numerical hypothesis tests and use the average mutual inclination as a statistic to select the distribution that fits well with the observation. Specifically, the null hypothesis is that δi follows the distribution of δi, according to the conditional probability in Equation (24) for each system. The null hypothesis can be rejected if the observed average δi, or values smaller than that, have a very small probability (<5%) under the null hypothesis.

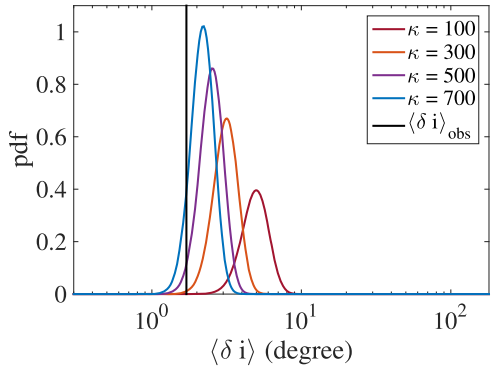

Figure 11. Probability distribution of the averaged mutual inclination, with different prior distribution of δi. The solid black line indicates the observed value.

We include four prior distributions, with four different κ: $\kappa = 100$, $\kappa = 300$, $\kappa = 500$, and $\kappa = 700$. We calculated the convolved distribution of the observed systems to obtain the distribution of $\langle\delta i\rangle$. The results are shown in Figure 11. The solid black line indicates the observed averaged mutual inclination. For the four prior distributions, the averaged mutual inclinations are $7\overset{\circ}{.}2$, $4\overset{\circ}{.}1$, $3\overset{\circ}{.}2$, and $2\overset{\circ}{.}7$, and the standard deviations are $3\overset{\circ}{.}8$, $2\overset{\circ}{.}2$, $1\overset{\circ}{.}7$, and $1\overset{\circ}{.}4$. The probability that the average mutual inclination is smaller than the observed value is 5×10^{-4}%, 0.19%, 2.2%, and 8.8% for $\kappa = 100$, $\kappa = 300$, $\kappa = 500$, and $\kappa = 700$, respectively. Thus, the hypothesis can be rejected when $\kappa = 100$, $\kappa = 300$, and $\kappa = 500$. In addition, it indicates that the mutual inclination distribution is more consistent with the observation for $\kappa > 500$, corresponding to an average mutual inclination of $\lesssim 3^\circ$.

The near co-planar ($\lesssim 3^\circ$) feature of the circumbinary planetary system is consistent with the coplanarity of the multi-transiting planetary systems with a single star (multis), where the study of transit duration ratios (Fang & Margot 2012; Fabrycky et al. 2014) and population synthesis studies (Moriarty & Ballard 2015; Ballard & Johnson 2016) suggest that most of the multis have mutual orbital inclinations less than $\sim 3^\circ$. Moreover, the observed circumbinary protoplanetary disks are also quite aligned with the stellar orbits ($\lesssim 3^\circ$) (Rosenfeld et al. 2012; Czekala et al. 2015, 2016), and this may indicate that the coplanarity of the circumbinary planets are primordial. In addition, based on the abundance studies by Armstrong et al. (2014) and Martin & Triaud (2014), the co-planarity of the circumbinary systems may indicate that the occurrence rate of the circumbinary systems is similar to that of single-star systems.

4.3. Multis versus Singles

Although nine out of the ten observed transiting circumbinary systems are single-transiting systems, it does not necessarily mean that circumbinary systems more likely contain a single planet, because farther companions are more difficult to detect via the transit method. In this section, we take into account the selection effects and investigate the multiplicity and planet–planet spacing of the planetary systems.

The transit probability of the outer companion is sensitive to its location, as the transit probability decreases with star-planet separation. On the other hand, outer companions of circumbinary planets cannot be located very close to the inner planets, because closely separated planets are unstable due to planet–

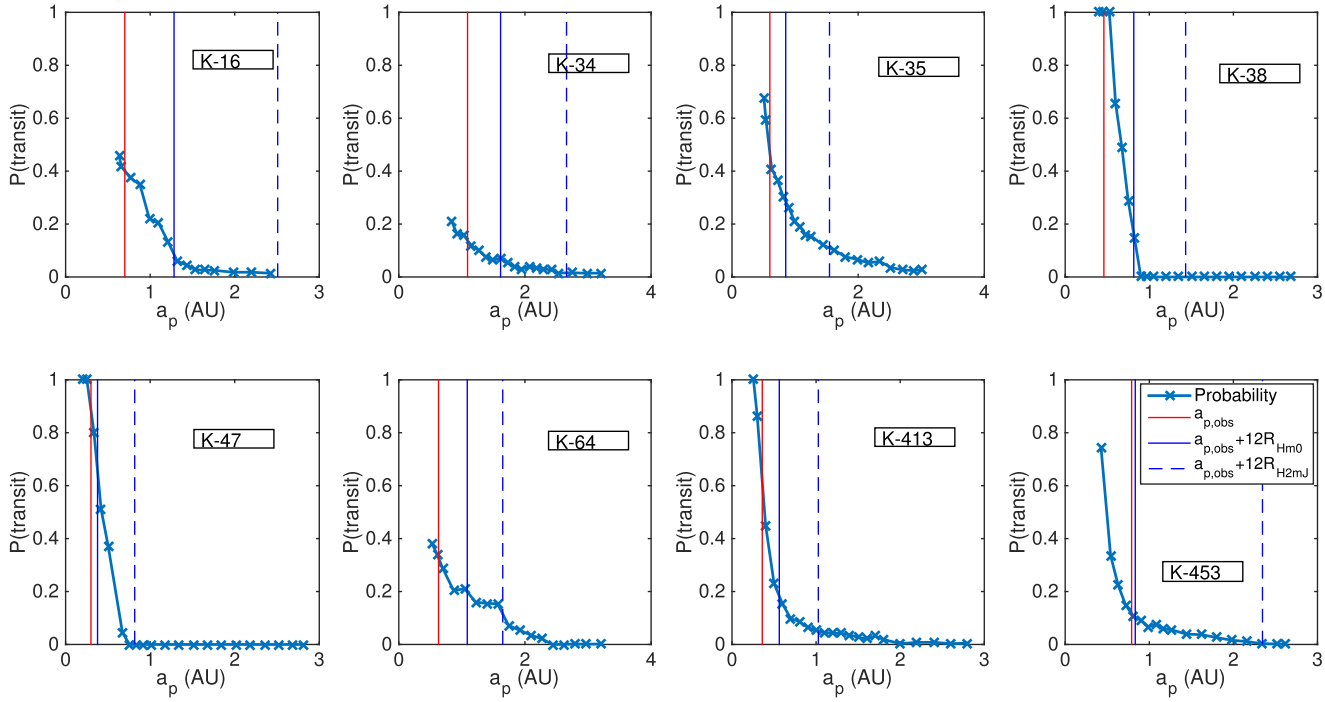

Figure 12. Probability that a planet transits at least twice, as a function of a_p for the observed systems. The red line indicates the location of the observed innermost planet. The solid blue line indicates the location of a companion test particle at 12 mutual Hill radii away from the innermost planet, and the dashed blue line indicates the location when the mass of the companion is two Jupiter masses.

planet interactions. It has been found that the observed spacing of the *Kepler* systems is clustered around ∼12 mutual Hill radii ($R_{\rm H}$), and it coincides with the required spacing for stability obtained using *N*-body simulations (e.g., Pu & Wu 2015). Dynamics of multi-planet circumbinary systems have been investigated by Kratter & Shannon (2014) and Smullen et al. (2016). In particular, it was found that the intra-planet spacing is of order 5–7$R_{\rm H}$ when the inner planet is close to a_c, and the spacing of the planet for the binary-case asymptotes to the single star results when the inner planet is farther ($a_p \sim 1.5$–$2a_c$). For simplicity, we mark the location of the outer companion at $12R_{\rm H}$ for illustration. The mutual Hill radius of the single stellar system is expressed as $R_{\rm H,single} = (a_1 + a_2)/2 \times ((m_{p,1} + m_{p,2})/(3M_*))^{1/3}$, where a_1 & a_2 and $m_{p,1}$ & $m_{p,2}$ are the semimajor axes and the masses of the planets, and M_* is the mass of the host star. For the circumstellar system, we set the mutual Hill radius to be:

$$R_{\rm H} = \frac{a_1 + a_2}{2}\left[\frac{m_{p,1} + m_{p,2}}{3(m_1 + m_2)}\right]^{1/3}. \quad (26)$$

Because the mass of the companion planet is not known, we set the companion planet to be a test particle with mass zero to obtain the maximum transit probability when the planet separation is the smallest. We set the companion planet mass to be two Jupiter masses, to probe the minimum probability when the planet separation is larger.

Similar to the previous sections, we require the planet to transit at least twice for a robust detection criterion. We then calculate numerically the probability to transit at least twice at different semimajor axes for the observed systems, assuming the the companion planets share the same mutual inclination with the innermost planet. A small probability at $a_p \gtrsim 12R_{\rm H}$ implies that it is unlikely to detect the companion, and thus it is possible to have farther undetected companions in the system.

The results are shown in Figure 12. The solid red line indicates the semimajor axis of the observed planet, and the solid (dashed) blue line represents the semimajor axis at 12 $R_{\rm H}$ away from the detected planet, assuming the companion planet has mass zero (two Jupiter masses). Note that, for Kepler-1647, the planet's orbital period is longer than 1470 days (∼four years) at 12 mutual Hill radii away, even when the companion is a test particle, so the probability to transit at least twice is zero. Thus, we exclude Kepler-1647 in the figure. Figure 12 shows that the probability to detect the outer companion is quite low, except for Kepler-47, if the planet mass is low. It is consistent with the observation where Kepler-47 indeed has multiple planets. Thus, we find no strong evidence that the circumbinary systems are more likely to contain a single planet.

4.4. Stellar Binary Period

It has been shown that the observed transiting circumbinary planets orbit around stellar binaries with long orbital periods ($\gtrsim$7 days) (e.g., Armstrong et al. 2014; Martin & Triaud 2014). However, a large number of eclipsing binaries have short orbital periods ($\lesssim$3 day) (e.g., Slawson et al. 2011). The absence of circumbinary systems may indicate that it is difficult to form planets around short-period binaries. In addition, this absence could be caused by the Lidov–Kozai mechanism, which contributes to the formation of short-period binaries. Specifically, short-period stellar binaries are formed through the Lidov–Kozai mechanism, and their inclination and eccentricity oscillate due to the perturbation of a third companion (Mazeh & Shaham 1979; Fabrycky & Tremaine 2007; Naoz 2016; Naoz & Fabrycky 2014). Note that the planet does not cause Lidov–Kozai oscillations in the stellar binary because it is not massive enough, as studied by

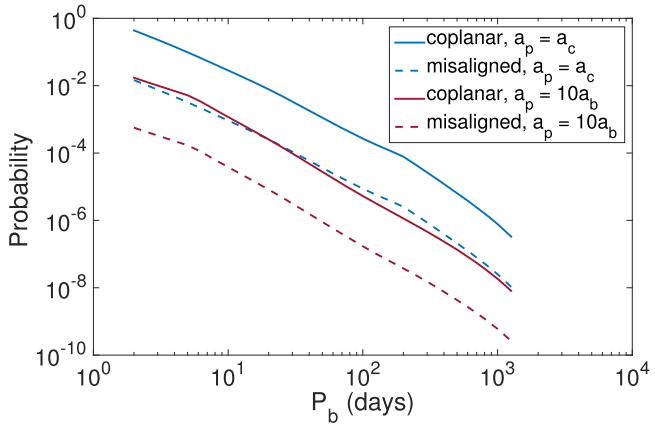

Figure 13. Probability to transit at least once for different stellar binary periods (P_b). The solid lines represent the near-coplanar case, and the dashed lines represent the highly misaligned case. The blue color represents the case when the planet is at the stability limit, and the red color represents the case when $a_p = 10a_b$, motivated by the Lidov–Kozai mechanism. The misaligned short-period stellar binary transit probability is similar to that of the aligned case when the planet is close to the star, but the probability decreases when the planet is farther.

Migaszewski & Goździewski (2011) and Martin & Triaud (2016), where the third companion, which produces the short-period binaries, needs to be massive. During this process, planets can be ejected or collide with the star, and the surviving planets end up having inclined orbits, with respect to the stellar orbit, to avoid transits (Martin et al. 2015; Muñoz & Lai 2015; Hamers et al. 2016). However, with precession, the transit probability at high mutual inclination can still be large. In this section, we study the probability distribution of the stellar binary orbital period including the misaligned cases.

First, we use the analytical result from Section 3 to obtain the transit probability, where, for simplicity, we set the stellar properties to those of the Sun, and we set the stellar binary to be aligned with the line of sight. We next set the prior period distribution of the eclipsing binary to be that of the *Kepler* sample. We integrate the probability over the mutual inclination, and obtain the probability distribution of P_b jointly with the event that the planet transits at least once. Specifically,

$$P(P_b \bigcap tt_1) = P(P_b)\left(\int P(tt_1|\delta i', P_b)P(\delta i')\, d\delta i'\right), \quad (27)$$

where tt_1 represents the event that the planet transits at least once in four years.

To compare the coplanar and the misaligned cases, we include a near-coplanar distribution $\delta i \lesssim 3°$, as discussed in Section 4.2, and a highly misaligned distribution $\delta i \in [40°, 140°]$, motivated by the Lidov–Kozai formation mechanism. For the case when the mutual inclination is less than 3°, we use the Fisher distribution with $\kappa = 500$; for the case when the mutual inclination is high, we set the distribution to be $P(\delta i) \propto \sin(\delta i)$, with lower and upper bounds of 40° and 140°, respectively.

Figure 13 shows the result. The solid lines represent the coplanar case, and the dashed lines represent the misaligned case. In addition, the blue lines indicate the case that $a_p/a_c = 1$, and the purple lines indicates the case when $a_p/a_b = 10$, motivated by the Lidov–Kozai mechanism, where the inner binaries shrink during the formation of the short period systems —and thus, the semimajor axis ratio of the planet to the stellar binary increases. We set the minimum P_b to be two days because the S/N level is lower when the stellar binary orbital period is shorter, and we set the maximum P_b to be four years. A detailed study on the short period limit due to the S/N level is important, but is beyond the scope of this article. Note that, because we set the stellar binary to be aligned with the line-of-sight, the actual transit probability for the coplanar case should be moderately lower than the results shown in Figure 13 when $\Delta_{ib} \neq 0$.

Taking into account the abundance of short-period binaries, the transit probability for the high mutual inclination, short-period stellar binary is similar to that of the aligned long stellar period case, when the planets locate near the stability limit. However, the planetary-to-stellar semimajor axis ratio increases during the formation mechanism, through Lidov–Kozai oscillations, as the stellar binary orbit shrinks. The increase of a_p/a_b further reduces the transit probability. Therefore, the circumbinary planets around short-period stellar binaries are still unlikely to be detected through the transit method. In other words, the formation mechanisms involving the Lidov–Kozai mechanism are consistent with the observations. This also implies that the planets probably do not move closer to the stellar binaries after the formation of the short period stellar binaries.

Although using transit methods it is unlikely to detect the misaligned circumbinary planets at distances far from the short-period stellar binaries, these planets can be detected through the eclipsing timing variation method. As the center mass of the stellar binary moves around the barycenter of the system, it causes variations in the light travel time from the stellar binary to the observer (e.g., Schneider & Doyle 1995; Schwarz et al. 2011). For hot Jupiters orbiting solar-type stellar binaries at 1 AU, this effect causes a time variation of the eclipses at the scale of 1 s; this is detectable using *Kepler* for a 9 mag target (Sybilski et al. 2010). The effect is stronger when the stellar mass is lower, and when the planets are farther away yet with periods shorter than the observation time.

5. CONCLUSIONS

In this paper, we investigate the architectural properties of planetary systems corrected by selection effects. First, we revisit the planetary stability limit when the planetary orbit is misaligned with the stellar binary. We find that the system is more stable when the mutual inclination is higher, which is consistent with Doolin & Blundell (2011), and we find that variations in the semimajor axes of the planets show interesting patterns. Next, we derive the analytical expression for the transit probability in a realistic setting, where a finite observation period and planetary orbital precession are both included. The analytical results agree well with the numerical simulations. In particular, the probability to transit one of the binary stars is shown in Equation (19), and the probability to transit both stars is shown in Equation (20). Different from the case with infinite observation time period (Martin & Triaud 2015), the transit probability does not always increase as a function of mutual inclination (as shown in Figure 7). In addition, comparing the transit probabilities of the circumbinary systems and systems with a single star, the transit probability for circumbinary systems can be lower if the observation period is very short (e.g., ~30 days, when $P_b = 5$ days, $a_p/a_b = 5$, and $\delta i \gtrsim 50°$). Thus, the transit probability of some circumbinary planets may be lower than their single-star

counterparts for the *TESS* mission, especially when the mutual inclination is high. On the other hand, the transit probability for the circumbinary planets is likely higher for the *K2, PLATO,* and *Kepler* missions.

Using the transit probability, we obtain architectural properties of the circumbinary systems. First, we study the distribution of planetary semimajor axes. Nine out of the ten observed circumbinary systems host innermost planets moderately close to the stability limit. However, the ninth system (Kepler-1647) hosts a planet that is much farther from the stability limit. Assuming that the tenth system is from a different distribution, there is only a small probability that the pile-up of planets near the stability limit is due to selection bias for the nine systems. This implies the dominance of migration during planet formation for a population of the circumbinary planetary systems. On the other hand, assuming that Kepler-1647 is in the same distribution, then, there is no strong evidence for a pile-up of planets near the stability limit. Observations of more circumbinary planetary systems can help distinguish these two scenarios. Moreover, we find that the pile-up is consistent with a log-uniform distribution of the planetary semimajor axis.

We next study the distribution of the mutual inclination between the planetary orbits and the orbits of the stellar binaries. All of the observed circumbinary planets to date are near-coplanar with the stellar orbits. The mutual inclination between the planet orbit and the stellar binary is much smaller than the result of an isotropic distribution, after taking into account the selection effects. We find that the mutual inclination can be fit well with a Fisher distribution of $\kappa \gtrsim 500$, corresponding to a average mutual inclination of $\lesssim 3^\circ$. This is similar to the mutual inclination for the multi-transiting systems around single stars (Fang & Margot 2012; Fabrycky et al. 2014; Moriarty & Ballard 2015; Ballard & Johnson 2016). Because the circumbinary protoplanetary disks also align with the stellar orbits within $\sim 3^\circ$ (Rosenfeld et al. 2012; Czekala et al. 2015, 2016), this may indicate a primordial alignment of the circumbinary planetary orbits.

Current observation seems to suggest that only one out of the ten observed circumbinary planetary systems hosts multiple planets. This can either be a result of the selection effects or imply that circumbinary planetary systems tend to host a single planet. To investigate this, we find that the probability to detect outer companion is very small for most of the systems, assuming a separation of $\sim 12 R_{\rm H}$ for stability purposes. Thus, we do not find strong evidence that the circumbinary planetary systems preferentially host a single planet. This indicates that the observed systems may have outer companions, but it is difficult to detect them.

Finally, we investigate the transit probability of systems with short-period stellar binaries and with inclined planetary orbits, motivated by the lack of observed circumbinary planets around short-period stellar binaries. We find that, considering the period distribution of eclipsing binaries, the transit probability of the misaligned system is similar to that of the aligned long stellar period systems, if the planet is located near the stability limit. However, the transit probability decreases as the planetary-to-stellar semimajor axis ratio decreases. This shows that the observation is consistent with the formation mechanism involving Lidov–Kozai oscillation, where the mutual inclination is excited and the semimajor axis ratio is reduced if the planet survives during the formation process (Martin et al. 2015; Muñoz & Lai 2015; Hamers et al. 2016). It also implies that the planets do not move closer to the stellar binary after the misalignment. Instead of transit methods, eclipsing time variation may provide a way to detect such circumbinary planets with misaligned, large semimajor axis ratios.

The authors would like to thank the anonymous referee for giving constructive comments that substantially improved the quality of this paper. In addition, the authors would like to thank Yanqin Wu and Josh Winn for helpful discussions. This work and M.T. were supported in part by NSF DMS-1521667. G.L. was supported in part by Harvard William F Milton Award.

REFERENCES

Armstrong, D. J., Osborn, H. P., Brown, D. J. A., et al. 2014, MNRAS, 444, 1873
Ballard, S., & Johnson, J. A. 2016, ApJ, 816, 66
Borucki, W. J., & Summers, A. L. 1984, Icar, 58, 121
Bromley, B. C., & Kenyon, S. J. 2015, ApJ, 806, 98
Cumming, A., Butler, R. P., Marcy, G. W., et al. 2008, PASP, 120, 531
Czekala, I., Andrews, S. M., Jensen, E. L. N., et al. 2015, ApJ, 806, 154
Czekala, I., Andrews, S. M., Torres, G., et al. 2016, arXiv:1601.03806
Dong, S., & Zhu, Z. 2013, ApJ, 778, 53
Doolin, S., & Blundell, K. M. 2011, MNRAS, 418, 2656
Doyle, L. R., Carter, J. A., Fabrycky, D. C., et al. 2011, Sci, 333, 1602
Dvorak, R., Froeschle, C., & Froeschle, C. 1989, A&A, 226, 335
Fabrycky, D. C., Lissauer, J. J., Ragozzine, D., et al. 2014, ApJ, 790, 146
Fabrycky, D., & Tremaine, S. 2007, ApJ, 669, 1298
Fabrycky, D. C., & Winn, J. N. 2009, ApJ, 696, 1230
Fang, J., & Margot, J.-L. 2012, ApJ, 761, 92
Farago, F., & Laskar, J. 2010, MNRAS, 401, 1189
Forest, E. 1989, in AIP Conf. Proc. 184, Physics of Particle Accelerators (Melville, NY: AIP), 1106
Foucart, F., & Lai, D. 2013, ApJ, 764, 106
Foucart, F., & Lai, D. 2014, MNRAS, 445, 1731
Fressin, F., Torres, G., Charbonneau, D., et al. 2013, ApJ, 766, 81
Hamers, A. S., Perets, H. B., & Portegies Zwart, S. F. 2016, MNRAS, 455, 3180
Hinse, T. C., Haghighipour, N., Kostov, V. B., & Goździewski, K. 2015, ApJ, 799, 88
Holman, M. J., & Wiegert, P. A. 1999, AJ, 117, 621
Howard, A. W., Marcy, G. W., Bryson, S. T., et al. 2012, ApJS, 201, 15
Katz, B., Dong, S., & Malhotra, R. 2011, PhRvL, 107, 181101
Kennedy, G. M., Wyatt, M. C., Sibthorpe, B., et al. 2012a, MNRAS, 421, 2264
Kennedy, G. M., Wyatt, M. C., Sibthorpe, B., et al. 2012b, MNRAS, 426, 2115
Kley, W., & Haghighipour, N. 2014, A&A, 564, A72
Kostov, V. B., McCullough, P. R., Carter, J. A., et al. 2014, ApJ, 784, 14
Kostov, V. B., McCullough, P. R., Hinse, T. C., et al. 2013, ApJ, 770, 52
Kostov, V. B., et al. 2015, arXiv:1512.00189
Kozai, Y. 1962, AJ, 67, 591
Kratter, K. M., & Shannon, A. 2014, MNRAS, 437, 3727
Li, G., Naoz, S., Holman, M., & Loeb, A. 2014, ApJ, 791, 86
Li, G., & Winn, J. N. 2016, ApJ, 818, 5
Lidov, M. L. 1962, P&SS, 9, 719
Martin, D. V., Mazeh, T., & Fabrycky, D. C. 2015, MNRAS, 453, 3554
Martin, D. V., & Triaud, A. H. M. J. 2014, A&A, 570, A91
Martin, D. V., & Triaud, A. H. M. J. 2015, MNRAS, 449, 781
Martin, D. V., & Triaud, A. H. M. J. 2016, MNRAS, 455, L46
Marzari, F., Thebault, P., Scholl, H., Picogna, G., & Baruteau, C. 2013, A&A, 553, A71
Mazeh, T., & Shaham, J. 1979, A&A, 77, 145
McLachlan, R. I., & Quispel, G. R. W. 2002, AcNum, 11, 341
Migaszewski, C., & Goździewski, K. 2011, MNRAS, 411, 565
Moriarty, J., & Ballard, S. 2015, arXiv:1512.03445
Muñoz, D. J., & Lai, D. 2015, PNAS, 112, 9264
Musielak, Z. E., Cuntz, M., Marshall, E. A., & Stuit, T. D. 2005, A&A, 434, 355
Naoz, S. 2016, ARA&A, 54, 441
Naoz, S., & Fabrycky, D. C. 2014, ApJ, 793, 137

Naoz, S., Farr, W. M., Lithwick, Y., Rasio, F. A., & Teyssandier, J. 2011, Natur, 473, 187
Orosz, J. A., Welsh, W. F., Carter, J. A., et al. 2012a, ApJ, 758, 87
Orosz, J. A., Welsh, W. F., Carter, J. A., et al. 2012b, Sci, 337, 1511
Paardekooper, S.-J., Leinhardt, Z. M., Thébault, P., & Baruteau, C. 2012, ApJL, 754, L16
Palacián, J. F., & Yanguas, P. 2006, CeMDA, 95, 81
Petigura, E. A., Marcy, G. W., & Howard, A. W. 2013, ApJ, 770, 69
Pierens, A., & Nelson, R. P. 2013, A&A, 556, A134
Pilat-Lohinger, E., Funk, B., & Dvorak, R. 2003, A&A, 400, 1085
Pu, B., & Wu, Y. 2015, ApJ, 807, 44
Rafikov, R. R. 2013, ApJL, 764, L16
Rosenfeld, K. A., Andrews, S. M., Wilner, D. J., & Stempels, H. C. 2012, ApJ, 759, 119
Schneider, J. 1994, P&SS, 42, 539
Schneider, J., & Doyle, L. R. 1995, EM&P, 71, 153
Schwamb, M. E., Orosz, J. A., Carter, J. A., et al. 2013, ApJ, 768, 127
Schwarz, R., Haghighipour, N., Eggl, S., Pilat-Lohinger, E., & Funk, B. 2011, MNRAS, 414, 2763
Silburt, A., Gaidos, E., & Wu, Y. 2015, ApJ, 799, 180
Silsbee, K., & Rafikov, R. R. 2015, ApJ, 808, 58
Slawson, R. W., Prša, A., Welsh, W. F., et al. 2011, AJ, 142, 160
Smullen, R. A., Kratter, K. M., & Shannon, A. 2016, arXiv:1604.03121
Sutherland, A. P., & Fabrycky, D. C. 2015, arXiv:1511.03274
Suzuki, M. 1990, PhLA, 146, 319
Sybilski, P., Konacki, M., & Kozłowski, S. 2010, MNRAS, 405, 657
Tao, M., & Owhadi, H. 2016, IJNA, 36, 80
Verrier, P. E., & Evans, N. W. 2009, MNRAS, 394, 1721
Welsh, W. F., Orosz, J. A., Carter, J. A., et al. 2012, Natur, 481, 475
Welsh, W. F., Orosz, J. A., Short, D. R., et al. 2015, ApJ, 809, 26
Wiegert, P. A., & Holman, M. J. 1997, AJ, 113, 1445
Winn, J. N., & Fabrycky, D. C. 2015, ARA&A, 53, 409
Yoshida, H. 1990, PhLA, 150, 262
Youdin, A. N. 2011, ApJ, 742, 38